ON THE USAGE OF TIP APPENDAGES FOR FLOW CONTROL IN AIR-COOLED CONDENSERS

Lorenzo TIEGHI[1*], Alessandro CORSINI[1], Giovanni DELIBRA[1], Johan van der SPUY[2], Francesco Aldo TUCCI[1]

[1]Department of Mechanical and Aerospace Engineering, Faculty of Industrial and Civil Engineering, Sapienza University of Rome, Rome, Italy.
[2]Department of Mechanical & Mechatronic Engineering, Faculty of Mechanical Engineering, Stellenbosh University, Cape Town, South Africa
*Corresponding Author, e-mail: lorenzo.tieghi@uniroma1.it. Tel.: +39 06 445 85234

ABSTRACT

Air cooled condensers (ACCs) are commonly found in power plants working with concentrated solar power or in steam power plants operated in regions with limited water availability. In ACCs the flow of air is driven toward the heat exchangers by axial fans that are characterized by large diameters and operate at very high mass flow rates near-zero static pressure rise. Given the overall requirements in steam plants these fans are subjected to inflow distortions, unstable operations and have high noise emissions.
Previous studies show that leading edge bumps in the tip region of axial fans effectively reduce the sound pressure levels without affecting the static efficiency of the fan. Nevertheless, the effects of such treatment in terms of flow patterns and heat exchanging in the whole ACC system were not investigated.
In this work, the effect of leading-edge bumps on the flow patterns is analyzed. Two RANS simulations were carried out using OpenFOAM on a simplified model of the air-cooled condenser. The fans are simulated using a frozen rotor approach. Turbulence modelling relies on the RNG k-epsilon model. The fan is characterized by a diameter of 7.3 m and a 333 m³/s of volumetric flow rate at the design point. The presence of the heat exchanger is modelled using a porous media approach.
The comparison between the flow fields clearly exert that the modified blade is responsible for the redistribution of radial velocities in the rotor region. This drastically reduces the losses related to the installation of the fan in a real configuration.
Keywords: air cooled condensers, CFD, flow control, inflow distortion, leading edge appendages.

NOMENCLATURE

ACC		Air-Cooled Condenser
P	[kW]	Fan power
Q	[m³/s]	Volume flow rate
U	[m/s]	blade velocity
c	[m/s]	absolute velocity
w	[m/s]	relative velocity
Δp_{TTS}	[Pa]	total-to-static pressure rise

Subscripts and Superscripts

r	radial
x	axial

1. INTRODUCTION

Condensers in steam power plants can be either water- or air- cooled. Usually, the first solution is preferred because it guarantees higher overall efficiency given the lower ancillary operational costs involved and a more compact solution. However, some power plants require air-cooled condensers, usually because of the lack of cooling water near the installation site. That is the case of concentrated solar power (CSP) plants with a bottoming Rankine cycle, as CSP are commonly installed in desertic areas, or large steam plants like [1], that are installed in desertic areas near largely populated cities.

For this work, we will refer to air-cooled condensers (ACC) and their typical arrangement and in particular to the design of fans inside these units. The ACC assembly comprises a series of cooling units (>400 in the plant shown in Figure 1) where large axial fans feed fresh air to a series of heat exchangers, where the steam condensates. The

typical arrangement, shown in, is that of a A-frame condenser unit with the fan inlet placed several meters above the ground and the heat exchangers on top of the fan.
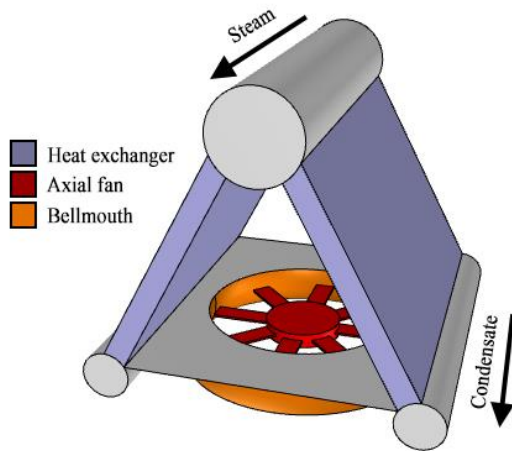

Figure 1: A-frame arrangement for an ACC unit

These fans are operated with very high-volume flow rates (250 to 400+ m³/s) and very low static pressure rise (100 to 300 Pa). This unusual combination results in a design characterized by large diameter (6-12m), low hub ratio (0.25-0.4) and rotational velocity between 100-200 rpm. Being so large and mounted on very high (>30m) structures to provide a sufficiently wide inflow, these fans are often characterized by a large and irregular tip clearance due to assembly issues that eventually reflect on fan efficiency [2].

Operations of these fans is also critical as efficiency drops when working with a lateral wind condition, in sandy environments or with extreme environmental temperature. In these conditions, the volume dilatation of the structures can in fact impact significantly on tip gap, with possible effects on fan efficiency, vibrations, mechanical failures, and noise emissions. Noise is in fact among the problems of large ACCs array due to the high number of fans involved [3][4].

Among the possible strategies available to fan designers to tackle part of these problems, sinusoidal serrations were proposed to control trailing edge separation, evolution of the tip leakage vortex and control noise. Developed from biomimicry assumptions on the hydrodynamics of the humpback whale fin tubercles [5], this leading edge modifications were found to change the dynamics of separation and loss of lift capability in NACA 4 digit modified airfoils. This capability derived by the counter-rotating vortices shed from the serrations at the leading edge, that at very high angles of attack (where the airfoil is supposed to operate in stalled conditions) result in controlling trailing edge separation and limiting it in span-wise positions that correspond to the trough of the leading edge

serration. Later studies, based on unsteady computations, revealed that a secondary motion arises in spanwise direction, with secondary phenomena resulting in a secondary shedding frequency that involves the whole blade span [6]. The separation control capability of leading edge serrations was exploited in modified axial fan geometries to control the development of the tip leakage vortex along the suction side of the rotor, resulting in a controlled stall dynamics [7]. Moreover, when dealing with noise, experimental and numerical findings [8][9] show how sinusoidal leading edges results in a change of the acoustic signature of the fan.

In the framework of H2020 MinwaterCSP project [10], we designed a fan for ACC that is now in operations at Stellenbosh University. This fan is running in an ACC unit in real conditions and is characterized by limitations that during operations can result in distorted inflow conditions and reduction of the volume flow rate. In particular this is a consequence of the nearby university buildings and of a water channel that flows below the test rig. Among the MinwaterCSP requirements for this fan there was a request for a low noise design as in real ACCs the hundreds of units can in fact results in health issues for people and fauna. In this case, however, the real problem comes from the proximity of the university and the presence of staff and students. For these reasons and given the background on leading edge serrations mentioned above, we here present a preliminary study of the effects of the modified geometry on the aerodynamics of this fan.

2. NUMERICAL METHODOLOGY

2.1. Computational Domain

The computational domain is chosen based on the experimental apparatus that is described in [2]. It describes a full-scale A-type air cooled condenser [11]**Errore. L'origine riferimento non è stata trovata.**. This ACC experimental configuration include a grid downstream of the fan, that was modelled using a porous media.
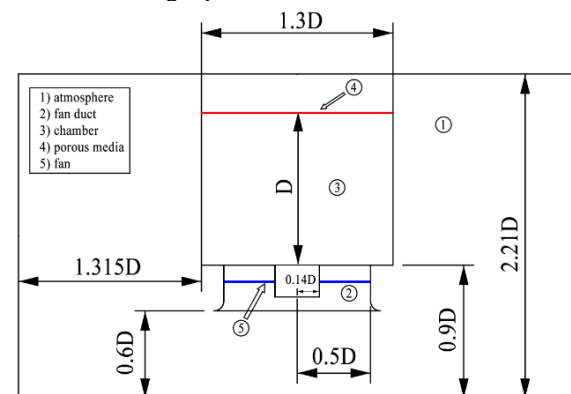

Figure 2 – Front view of the numerical domain

The structural supports to the exchanger are not included in the final model, their effect being neglectable from an aerodynamic point of view. The domain, normalized by the rotor diameter D, is reported in Figure 2.

The domain is symmetric with respect to the fan, therefore each of the four lateral boundaries is located at 1.315D from the exchanger walls.

2.1. Fan Description

The fan is an eight-blade low-speed axial fan. Rotor diameter is 7.3 m, with a hub-to-tip ratio equal to 0.284. Tip clearance is set to 0.2% of the blade tip chord. The rotational speed of the fan is 151 rpm. The fan provides 105 Pa of total-to-static pressure at the nominal volumetric flow rate of 333 m^3/s. The design process of both the fan and its modified version are reported in [12]. The leading edge bumps are designed by varying the blade chord of +/-5%, following a sinusoidal low in the last 25% of the blade span. The original blade, here labeled as *datum* fan, and its modified version, here labeled as *whale* fan, are shown in Figure 3.
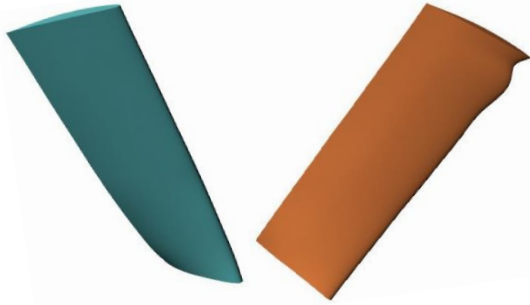

Figure 3 - Datum (left) and whale (right) fan geometries

2.3. Computational Grid

The computational grid was generated for both geometries using the *snappyHexMesh* utility of the OpenFOAM v2106 library. The base grid entails 0.8M cells with unity aspect ratio and a cell size of approximately 0.13m. The grid is sequentially refined in the whole exchanger and in the rotor region, as shown in Figure 4.

Due to the large computational domain, the grid was designed for high Reynolds computation. Therefore, the wall spacing was set to achieve a y$^+$=100 on the first layer of cells.

A grid sensitivity analysis on the datum fan configuration was performed using total-to-static pressure rise and convergence parameter. Results are shown in Figure 5, showing that a grid refinement of 20M cells is sufficient for this setup.

In particular, 2M cells are used to model the external atmosphere, 15M in the rotor region and 3M

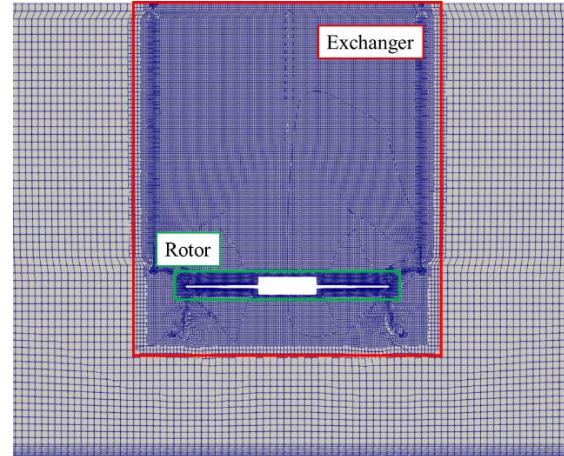cells in the exchanger. A visualization of the grids on the whale fan rotors is provided in Figure 6.
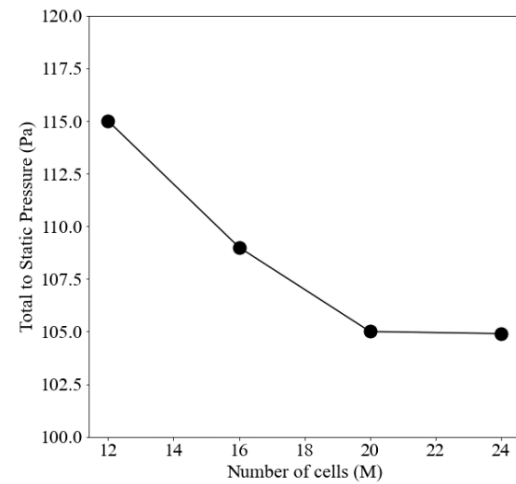

Figure 4 - Grid refinements

Figure 5 - TTS pressure as a function of the number of cells, datum blade

2.4. Porous media setup

The porous media is modelled using the parabolic Darcy-Forchheimer relationship. The 10 cm thick, porous region in the exchanger is responsible of a pressure loss that is calculated according to:

$$\frac{\partial p}{\partial x_j} = -\frac{\mu}{\kappa} U_j - \frac{\mu}{\kappa_1} U_j^2 \qquad (1)$$

where κ and κ_1 are respectively the Darcy and Forchheimer coefficients. This pressure gradient acts as sink term in the momentum equation. The coefficients of Eq. (1) where derived from the geometry of the squared grid in the test-rig that has a characteristic length of 5 cm, following the methodology reported in [13]. Since the flow is characterized by a predominant axial direction, the coefficients in orthogonal directions are set to 10^{10}.

2.5. Numerical setup

Turbulence modelling relies on the RNG k-epsilon model [14]. The steady computations are based on a frozen rotor approach and the incompressible equations are solved using the SIMPLE solver. Convergence was assessed by the torque of the fan and the velocity in probes up- and downstream of the fan. The linearized systems of equations were solved using a smoothSolver for all the quantities, except for pressure, that was solved using a conjugate gradient solver. Tolerance for convergence was set to 10^{-6} for all quantities except pressure, that was set to 10^{-4}.
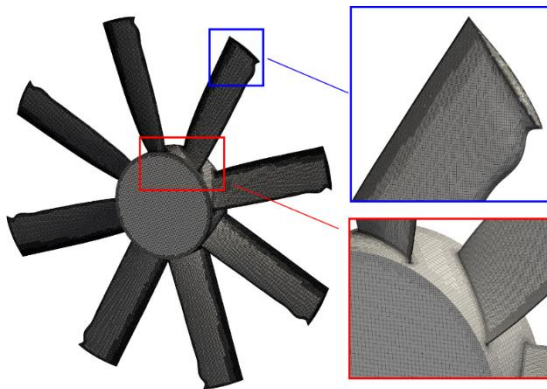

Figure 6 - Mesh of the fan and details of the grid at blade tip and hub, whale fan design2.6. Boundary conditions

A scheme of the boundary condition is reported in Figure 7. The terrain is treated as a rough wall, with relative thickness of 0.1. The mass flow rate is imposed on the lateral boundaries, equal to 25% of the duty point of the fan. Atmosphere is treated as a slip wall for numerical stability of the simulation. At the outflow of the fan, total pressure is imposed, with zeroGradient (zG) condition on velocity. On all solid surfaces, standard wall functions for turbulent kinetic energy, dissipation rate and turbulent viscosity are used.
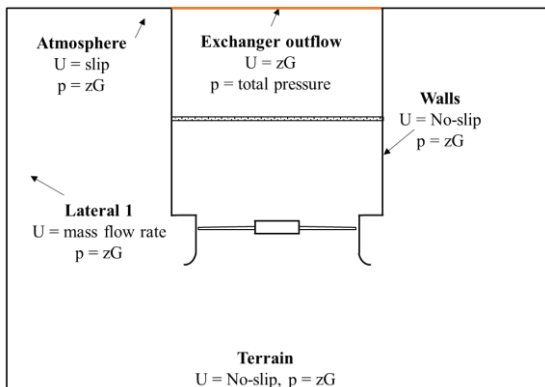

Figure 7 - Scheme of boundary conditions, front view

3. RESULTS

For a preliminary assessment of the accuracy of computations, a comparison of TTS pressure and TTS efficiency are shown in Table 1. Pressure is averaged over two planes at 1.6 D and 1.8 D from the terrain. Numerical computations results show that the pressure rise capability of the two fans in ISO conditions is practically the same, with slightly worst efficiency of the whale fan, confirming the conclusions in [15]. However, the installation inside the ACC setup leads to different behavior: the datum geometry in fact shows a reduction of the pressure rise capability of 32%, with a negligible change in power adsorbed, while the whale fan has a reduction of pressure rise capability and power consumption of about 10%.

Table 1. Validation of CFD results

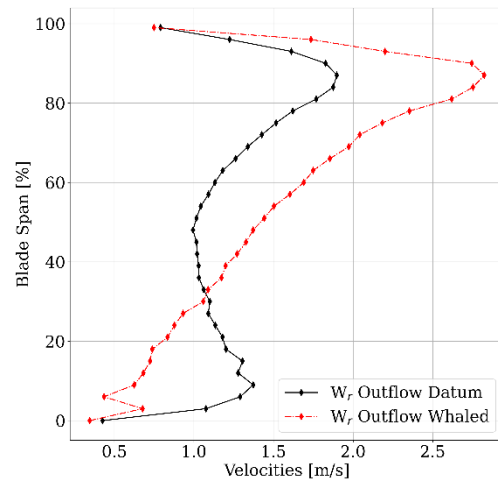| Arrangement		Q	Δp_{TTS}	Power
-	-	m³/s	Pa	kW
Datum	ACC	333	95	61.7
	Single Rotor	333	140	60.4
Whale	ACC	333	123.8	56
	Single Rotor	333	137.6	62

Figure 8 – Radial velocity at the outlet of the datum fan (black) and the whale fan (red)

This change in performance is associated to a higher work capability of the tip region and a change into the spanwise behavior of the flow. This is shown in Figure 8, where the whale fan shows a linear trend from root to 85% of the span, while the datum geometry has a higher radial velocity value at the root of the blade and then a lower value from 1/3 of the blade span.

The change in performance can be associated mainly to the effect of the leading-edge modification on the development of the tip leakage vortex. As shown in Figure 9 in fact at the through of the sinusoidal leading edge the flow accelerates and reaches a relative velocity of over 70 m/s. The

resulting jet released by this region of the rotor delays the development of the tip leakage vortex with respect to the datum fan. In fact, in the datum geometry the leaking starts at about 10% of the chord of the tip section, with a secondary vortex being released at about 50% of the chord.

On the whale rotor only this second structure is present, due to the counter rotating flow released by the modified leading edge that blocks the development of the first leaking structure.

This is better seen in Figure 10 and Figure 11 where relative velocity and pressure contours are plotted on an iso-radius surface at 99% of the blade span. In both figures the trace of the tip leakage vortex system is clearly recognizable, with a delayed development for the whale rotor geometry
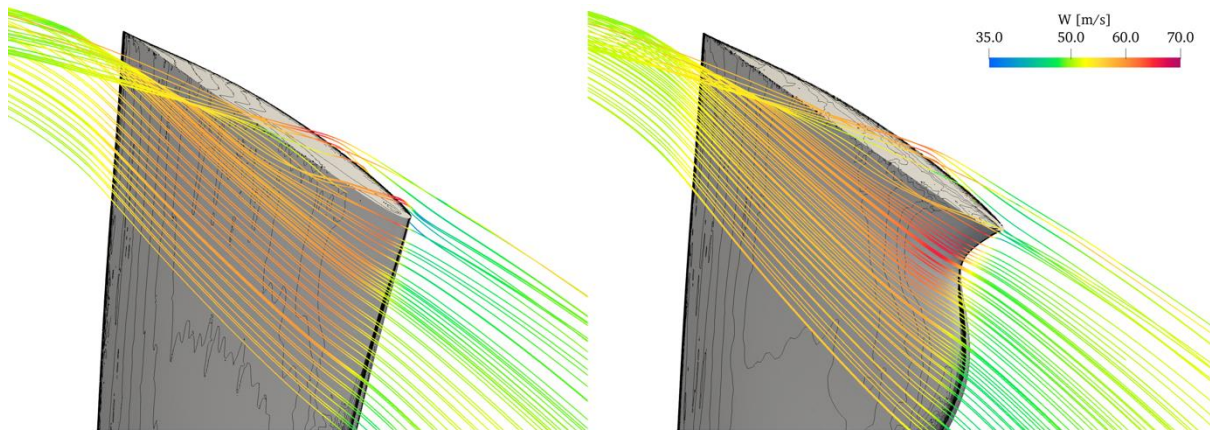

Figure 9 – Relative velocity streamlines on the tip region for datum (left) and whale (right) fan colored with relative velocity
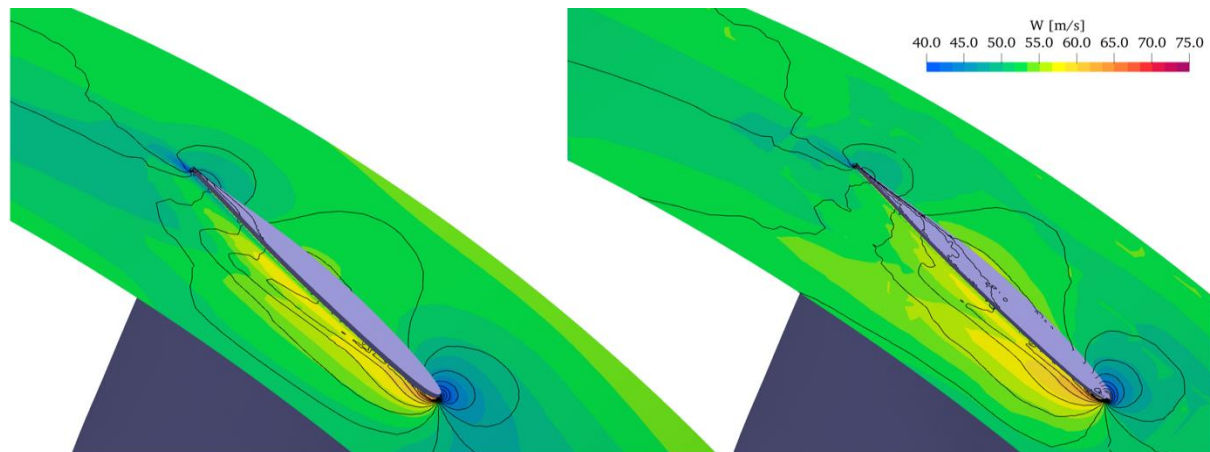

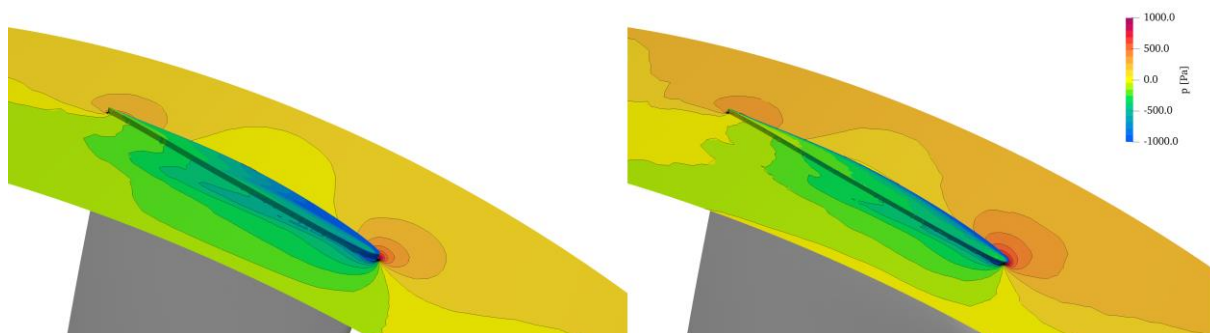**Figure 10 - Relative velocity contours on iso-radius surface at 99% of the blade span for datum (left) and whale (right) fan**

Figure 11 - Relative contours on iso-radius surface at 99% of the blade span for datum (left) and whale (right) fan

5. CONCLUSIONS

Following the conclusions of previous works on modified fan rotors with sinusoidal leading edges, we tested this flow control solution on an air-cooled condenser fan for steam power plants.

In ISO arrangements show that the original blade and the whale blade have similar performance in both total-to-static pressure rise capability and adsorbed power. When fitted in the ACC however there is a clear improvement as the whale fan have a loss of pressure rise with respect to the ISO arrangement that of about 11%, against a loss of 32% for the datum blade. Also, the absorbed power is reduced of 10% while the datum fan has negligible difference with respect to ISO conditions.

The different behavior was then related to a radial redistribution of the flow induced by the modified rotor and its capability to control and contrast the development of the tip-leakage vortex on the suction side of the rotor. These findings are similar to those shown in [5].

REFERENCES

[1] Fourie, N., Van Der Spuy, S. J., & Von Backström, T. W. (2015). Simulating the effect of wind on the performance of axial flow fans in air-cooled steam condenser systems. Journal of Thermal Science and Engineering Applications, 7(2), 021011.

[2] Van der Spuy, S. J., Els, D. N. J., Tieghi, L., Delibra, G., Corsini, A., Louw, F. G., ... & Meyer, C. J. (2021, June). Preliminary Evaluation of the 24 Ft. Diameter Fan Performance In the MinWaterCSP Large Cooling Systems Test Facility. In Turbo Expo: Power for Land, Sea, and Air (Vol. 84898, p. V001T10A005). American Society of Mechanical Engineers.

[3] Van der Spuy, S. J., von Backström, T. W., & Kröger, D. G. (2009). Performance of low noise fans in power plant air cooled steam condensers. Noise Control Engineering Journal, 57(4), 341-347.

[4] Angelini, G., Bonanni, T., Corsini, A., Delibra, G., Tieghi, L., & Volponi, D. (2018). On surrogate-based optimization of truly reversible blade profiles for axial fans. Designs, 2(2), 19.

[5] Corsini, A., Delibra, G., & Sheard, A. G. (2013). On the role of leading-edge bumps in the control of stall onset in axial fan blades. Journal of fluids engineering, 135(8).

[6] Zhang, M. M., Wang, G. F., & Xu, J. Z. (2013). Aerodynamic control of low-Reynolds-number airfoil with leading-edge protuberances. AIAA journal, 51(8), 1960-1971.

[7] Corsini, A., Delibra, G., & Sheard, A. G. (2014). The application of sinusoidal blade-leading edges in a fan-design methodology to improve stall resistance. Proceedings of the Institution of Mechanical Engineers, Part A: Journal of Power and Energy, 228(3), 255-271.

[8] Biedermann, T. M., Kameier, F., & Paschereit, C. O. (2019). Successive aeroacoustic transfer of leading-edge serrations from single airfoil to low-pressure fan application. Journal of Engineering for Gas Turbines and Power, 141(10).

[9] Biedermann, T. M., Chong, T. P., Kameier, F., & Paschereit, C. O. (2017). Statistical–empirical modeling of airfoil noise subjected to leading-edge serrations. AIAA Journal, 55(9), 3128-3142.

[10] The MinWaterCSP Project - http://www.minwatercsp.eu

[11] Kirstein, C., von Backström, T. and Kröger, D. (2005). Flow Through a Solar Chimney Power Plant Collector-to-Chimney Transition Section. International Solar Energy Conference. DOI: 10.1115/ISEC2005-76011.

[12] Volponi, D., Bonanni, T., Tieghi, L., Delibra, G., Wilkinson, M., van der Spuy, J. and von Backström, T. (2018). CFD Simulation Results for the MinWaterCSP Cooling Fan. DOI: 10.13140/RG.2.2.22031.89768.

[13] Idelchik, Isaak E. "Handbook of hydraulic resistance." wdch (1986)

[14] Yakhot, V. S. A. S. T. B. C. G., Orszag, S. A., Thangam, S., Gatski, T. B., & Speziale, C. (1992). Development of turbulence models for shear flows by a double expansion technique. Physics of Fluids A: Fluid Dynamics, 4(7), 1510-1520.

[15] Tieghi, L., Delibra, G., Corsini, A., & Van Der Spuy, J. (2020). Numerical investigation of CSP air cooled condenser fan. In E3S Web of Conferences (Vol. 197, p. 11010). EDP Sciences.